PCCP

Accepted Manuscript

ROYAL SOCIETY OF CHEMISTRY

www.rsc.org/pccp

Squeezing water clusters between graphene sheets: energetics, structure, and intermolecular interactions

S. McKenzie, *H.C. Kang

Department of Chemistry

National University of Singapore

Singapore

*e-mail: chmkhc@nus.edu.sg

Abstract

The behavior of water confined at the nanoscale between graphene sheets has attracted much theoretical and experimental attention recently. However, the interactions, structure, and energy of water at the molecular scale underpinning the behavior of confined water have not been characterized from first-principles. In this work we consider small water clusters up to the hexamer adsorbed between graphene sheets using density functional theory calculations with van der Waals corrections. We investigate the effects on structure, energy, and intermolecular interactions due to confinement between graphene sheets. For interlayer distances of about one nanometer or more, the cluster adsorption energy increases approximately linearly with cluster size by 0.1 eV per molecule in the cluster. As the interlayer distance decreases, the cluster adsorption energy reaches a maximum at 6 to 7 Å with approximately 0.16 eV stabilization relative to large interlayer distances. This suggests the possibility of controlling the amount of adsorption in graphene nanomaterials by varying the interlayer distance. We also quantify the intermolecular hydrogen bonding in the clusters by calculating the dissociation energy required to remove one molecule from each cluster. For each cluster size, this is constant for interlayer distances larger than approximately 6 to 8 Å. For smaller distances the intermolecular interaction decreases rapidly thus leading to weaker cohesion between molecules in a squeezed cluster. We expect a mechanism of concerted motion for hydrogen-bonded water molecules confined between graphene sheets, as has been observed for water confined within carbon nanotubes. Thus, the decrease in the dissociation energy we observed here is consistent with experimental results for water transport through graphene and related membranes that are of interest in nanofiltration. We also calculate the corrugation in the interaction potential between graphene which suggests a switch from very small corrugation to stick-slip behavior at interlayer distances smaller than 6 Å. Our results for gas phase clusters agree reasonably with methods using more demanding quantum chemical methods to treat the van der Waals interactions, thus providing support for the relatively fast density functional theory methods used here for studying water-graphene interactions in nanoscale systems.

Introduction

There is considerable interest in the properties of nanoscale-confined water molecules and their interactions with carbon nanostructures [1-13]. An early motivation was the discovery that water fills carbon nanotubes[1] and flows through nanotubes (with diameter 8.1 A)in an interesting single-file fashion at an exceptionally fast rate [2]. Similar results were also found more recently for carbon nanotubes with much larger diameters of about 7 nm [3, 4] On the other hand, results for smaller diameter (2 to 5 nm) multiwall carbon nanotubes showed that the mobility is greatly decreased. [5].Similarly, confinement of water between hydrophilic walls with separations less than about 1 nm increases its viscosity by seven orders of magnitude over the bulk [6] through cooperative hydrogen bonding to the surfaces, indicating the importance of hydrogen bonding close to the hydrophilic wall. Reduced translational and reorientational mobilities are also observed for confinement between graphene sheets at 1.3 nm or less [7].The interfacial structure of water confined between graphene sheets has also been examined using molecular dynamics, showing that liquid water molecules are arranged inlayer-by-layer structure close to the graphene, at least for sheets approximately 30 A apart [8-10]. The confinement-induced phase transition in this interfacial region with a hydrophobic surface has also been observed in other molecular dynamics simulations [11,12]. These, and related, phenomena are of broad fundamental relevance to understanding the interactions of water with graphene at the molecular level, and are potentially important in nanotechnology. For example, understanding water adsorption on graphene sheets is important in most material applications and it is a good model for assessing the potential of single-molecule detection through adsorption on graphene. More recently rapid transport of water through graphene oxide membranes has been observed [13]. In contrast these membranes are impermeable to small molecules such as He, H_2, N_2, and Ar. The selective transport of ions through graphene oxide membranes have also been reported [14, 15].Thus, there is significant potential for using graphene and graphene oxide membranes in separations technology. Apart from having great relevance to the flow of water through graphitic nanostructures, such work also provides insight for water transport through non-polar channels in biological systems [16].

Aside from these materials-related properties, it is also of interest to calibrate the interaction between confined water molecules and their interactions with the confining walls. This is a non-trivial combination of hydrogen bonding and van der Waals interaction, and it is interesting to see how various computational methods perform, and in particular, if they are sufficiently accurate and fast for investigating graphene-water systems at the nanoscale. Thus far, a number of molecular dynamics calculations have been done using classical potentials to study flow properties of somewhat large systems. Simulations with density-functional theory Born-Oppenheimer molecular dynamics but without correcting for van der Waals interaction have also been used to examine the structure of water confined by graphene [10]. In this work we consider adsorbed water clusters small enough to be accessible with van der Waals corrected density functional theory (vdw-DF) calculations [17, 18].Accurate calculation of van der Waals

interactions is an actively investigated field currently. We here list some of the most common techniques. The use of highly accurate quantum chemical methods such as coupled-cluster with single, double, and perturbative triple excitations (CCSD(T)) is too expensive and thus not feasible for the somewhat large systems such as liquid water in graphene oxide membranes. Several strategies have been explored for treating these long-range interactions. A common strategy is to use density functional theory within the generalized gradient approximation as a starting point, and correcting for van der Waals interactions using various methods. These include: adding a r^{-6} correction term with a coefficient determined empirically or by fitting to quantum chemical calculations[19-21];time-dependent density functional theory to treat the dispersion interactions [22, 23]; treating the long-range tail of the correlation functional as a density-density interaction that depends upon the electron density and its gradient [17, 18]. This last methodology explicitly accounts for van der Waals interactions through a simple, physically sound basis, and provides fast and reasonably accurate results. Using this last method we investigate in this work the properties of small water clusters adsorbed between graphene layers. We quantify the energy and structure of the adsorbed cluster and the intermolecular interactions within the clusters. We also calculate the gas-phase clusters in order to provide some validation for the methodology and to compare to the adsorbed state. We examine how the structure and energies change as the clusters are squeezed between graphene sheets.

Methodology

To simulate a multilayer system of graphene sheets, we use a hexagonal supercell with lateral dimensions of (5 x 5) unit cells of the graphene lattice with the usual AB stacking. The in-plane geometry is fixed to the one determined experimentally so that the C-C distance is 1.421 Å. In our production calculations the supercell length in the dimension perpendicular to the plane of the graphene sheets depends upon the interlayer distance; a supercell length of 26 Å perpendicular to the graphene sheets is used for an interlayer distance of 13 Å. Thus, each supercell contains two graphene sheets and includes two interlayer spaces between these sheets, and consists of 100 carbon atoms in addition to the water molecules. We perform mostly calculations with a water cluster in one of these interlayer spaces leaving the other vacant, so that in this work we are not considering the interactions of the water clusters through the graphene sheets. However, we also perform some calculations with water clusters in both of the interlayer spaces in order to assess the magnitude of the interactions on the adsorption energies. The calculations are performed with the Quantum-ESPRESSO ab initio package [24] using the vdW-DF [17] or vdW-DF2 [18] prescription for the non-local correlation energy along with different exchange functional following the approach in Ref. 25. We use three different density functionals for the exchange component: revised-Perdew-Burke-Ernzehof (rPBE) [26], Becke-Lee-Yang-Parr (BLYP) [27], and Perdew-Wang86 (PW86) [28] in combination with non-local correlation corrections [17, 18] above. We denote these methodologies below by the exchange correlation functionals, that is, vdw-DF(rPBE), vdw-DF2(BLYP), and vdw-DF2(PW86).

Ultrasoft pseudopotentials [29] are used to describe the carbon, oxygen, and hydrogen atoms, while norm-conserving potentials [30] are used for the calculations for adsorption of argon. We used cut-off energies of 40, 80, 100, and 120 Ry in our initial calibration to check for convergence with respect to wavefunction cutoff energy, and only 80 Ry for most of the other calculations. A density cutoff energy of 480 Ry is used for the 80 Ry wavefunction cutoff calculations. The convergence criteria used for geometry optimization are 10^{-5} Ry for total energy convergence and 10^{-4} Ry/bohr for force convergence. The band structure of graphene requires dense Brillouin zone sampling. However, previous work on adsorption of water on graphene in periodic supercell calculations have used the Γ point, and suggested that it is sufficient for a (5×5) supercell [31,32]. Nevertheless, we have calibrated this sampling using the adsorption energy of the water monomer by using n × n × 1, with n equal to 1, 2, 4, and 8 in a supercell with interlayer spacing of 15 Å. For each of these calculations, the adsorption energy of the (more stable) one-legged adsorbed geometry of the water monomer relative to the n=1 calculation is -0.231 meV, -0.202 meV, and -0.202 meV. respectively, for n=2, 4, 8. Thus, our calculations used 4×4×2 sampling for the production calculations, and in view of the smaller interlayer distance compared to the calibration calculations.

Results and discussion

Compared to the situation for liquid water calculations, the quantum chemical results for gas phase water clusters are considerably more consistent [33-38]. We examine and report results for gas-phase clusters in order to calibrate the vdw-DF methods used here and to assess the effect of adsorption upon the geometry of water clusters later. The interaction energy for gas phase clusters is calculated using $E_{int,N} = NE_1 - E_N$; results are summarized in the first row in each entry in Table 1 where N is the number of molecules in the cluster, E_1 and E_N are the total energy, respectively, for the monomer and the N-molecule cluster. This is the energy required to dissociate an N-molecule cluster into N gas-phase molecules. For the dimer, this gives the hydrogen bond strength between two water molecules. We find that the vdw-DF2 (PW86) methods can predict the correct relative stability of the hexamers in the gas-phase. For the hexamer, we examine the four stable structures – prism, cage, book, ring – using DF-vdW2 (PW86). Previous work [36-38] on the accuracy of density functional theory methods and dispersion corrections on hexamers is particularly relevant here. It has been shown that DFT exchange-correlation functionals without dispersion corrections do not correctly predict the relative stability of these structures [36]. In addition, non-dispersion error in PBE and BLYP functional overestimate distances between non-hydrogen bonded monomers [38], and these methods generally overestimate the charge transfer contribution to the interaction energy [37]. Thus, it is important to calibrate the relative energies of the hexamers using the vdw-DF methods to the more accurate quantum chemical approaches. In the gas phase, the lowest energy structures within 1 kcal/mol of each other are the prism, cage, book, and ring geometries. From ΔCCSD(T) calculations which extrapolate MP2 energies to complete basis set limit using the MP2 and CCSD(T) energy difference at the triple-zeta level [25], these structures require

energies (equal to the quantity $E_{int,6}/6$ in Table 1) of 334, 332, 329, and 321 meV, respectively, to dissociated into six gas phase water molecules. The vdw-DF2 (PW86) calculations give 348, 347, 346, and 338 meV, for the prism, cage, book, and ring, respectively. Thus, our calculations show that the vdw-DF2 (PW86) reproduces the correct energy ordering of more stable gas phase water hexamers. The rather small energy differences of the more expensive calculations are reproduced reasonably well. The dissociation energies from our calculations are within 14 to 17 meV of the ΔCCSD(T) values.

In order to compare structural results with previous calculations, the average O-H---O bond angle and the O-O distance are calculated for the hydrogen bonds in each cluster and compared to previous work reporting these parameters in Refs. 33 and 39. In order to pick out hydrogen bonds in the clusters it suffices to use the structural criteria that the O-H---O bond angleis greater than 140°, and the OH---O distance is between 1.5 Å and 2.5 Å.Results are shown in the second row in each entry in Table 1 and compared with the results from previous calculations [33, 39] where the same structural parameters were reported. The calculations in Ref. 39 use density functional theory with van der Waals corrections through dispersion-corrected atom-centered potentials (DCACP) [40], while Ref. 33 uses second-order perturbation theory (MP2)with augmented correlation-consistent double through quintuple zeta orbital basis sets to approximate the complete-basis set limit (CBS). The interaction energies obtained here are within 0.05 eV of the MP2-CBS calculations. The interaction energies predicted by vdw-DF and vdw-DF2 are all larger than the MP2-CBS results. The average bond lengths are within 0.15A of the DCACP results, although the average O-H---H bond angles differ by up to 6°. Compared to the DCACP calculations our calculations show a larger difference between the results for the BLYP and rPBEdensity functionals. This is probably because in our calculations we use the initially proposedvan der Waals correction [17] for the rPBE calculations, andthe refitted correction [18] for the BLYP calculations. Thus, the methodology used here produces structures and energies of water clusters in reasonable agreement with higher level quantum chemical calculations.

To facilitate our discussion on intracluster hydrogen bonding, it is interesting to consider the energy required to dissociate a N-molecule gas-phase cluster into the (N-1)-molecule gas-phase cluster plus a gas-phase water molecule $E_{diss,N} = E_{N-1} + E_1 - E_N$. This is the last value in each entry in Table 1. It is simply related to the interaction energy above through $E_{diss,N} = E_{int,N} - E_{int,N-1}$. As the cluster size N increases and approach the bulk liquid water structure, we expect $E_{diss,N}$ to increase because the number of hydrogen bonds per molecule increases. For the dimer dissociating to form two gas-phase molecules, $E_{diss,2}$ is the hydrogen bond strength between two adsorbed water molecules. We obtain values of 0.244, 0.238, and 0.214 eV, for the vdw-DF2 (PW86), vdw-DF2 (BLYP), and vdw-DF (rPBE) methods, respectively. The small clusters we investigate here are certainly not in the bulk regime and each, except for the compact prism, cage, and book hexamers, only has one hydrogen bond per molecule. It should be noted that $E_{diss,N}$ is not simply correlated to the change in the number of hydrogen bonds with dissociation. For instance, when the tetramer dissociates to form the trimer, the number of hydrogen bond

decreases by one although $E_{diss,N}$ is close to 0.5 eV, i.e. approximately twice the hydrogen bond strength from the $E_{diss,2}$value for the dimer. This is because the average strengths of the hydrogen bonds in these small clusters vary greatly with cluster size. The trimer bonds are probably particularly weak because of the angular strain in the hydrogen bond leading to a high $E_{diss,4}$ for the tetramer, and thus there is a decrease in the $E_{diss,N}$ value for the pentamer relative to the tetramer. This dip in$E_{diss,N}$ for the pentamer is interesting to examine more closely. It can be understood if we consider the bond angles between the hydrogen bond at each acceptor oxygen atom and its two O-H covalent bonds. For each of the clusters from the trimer to the hexamer, the values for these bond angles fall into two groups, one smaller and one larger value. The average values are, respectively, (90.1°, 126.2°), (103.4°, 121.7°),(112.2°, 121.1°), and (105.0°, 127.3°) from the trimer to the hexamer. This data shows that there is considerable deviation in the trimer bond angles from the tetrahedral angle compared to the tetramer and the pentamer. Thus, in going from the tetramer to the trimer these bond angles show a large increase in bond angle strain. On the other hand this is not the case for dissociating the pentamer. Hence, the energy cost in dissociating the tetramer to form the trimer is considerably larger than dissociating the pentamer to form the tetramer. We also observe an increase in $E_{diss,N}$ from the pentamer to the hexamers because, except for the ring structure, each hexamer has more than one hydrogen bond per water molecule. For the most stable adsorbed hexamer, the book structure, this is 7/6 hydrogen bonds per water molecule, compared to one per water molecule in the pentamer. Previous results reported in Refs. 33 and 39 also show this dip in $E_{diss,N}$ for the pentamer although it was not noted. The difference in dissociation energy values between our calculations and the results from MP2-CBS results are within 0.05 eV. In summary, the gas-phase cluster interaction energies, bond lengths and angles arising from hydrogen bonding appear to be well accounted for by the methodology we use here.

While adsorption of a single water molecule has been widely studied using first-principles calculations [31, 32, 40-42], there are few first-principles results for adsorbed clusters of water larger than the monomer. Born-Oppenheimer molecular dynamics simulations have been reported, a recent study [43] using BLYP functional with a van der Waals correction [44, 45], and another earlier study [46] using PBE functional with no van der Waals correction. Both these simulations used elevated temperatures in order to simulate room temperature behavior, indicating that the interaction potentials used can be improved. It is thus interesting to consider the influence of adsorption on the geometry and energy of the water clusters which are small enough to be treated with van der Waals corrected density functional methods. Here we discuss some new results related to the various minimum energy adsorption structures found in our calculations as this is of some general interest although our main aim in this work is to investigate the effect of squeezing these adsorbed water clusters. The stable minima we found are illustrated in Fig. 1 with top and perspective views. Previous investigations [31, 32, 40-42] have examined two minimum energy structures for the adsorbed monomer. We consider both in our calculations, the first with a single hydrogen atom and the second with both hydrogen atoms pointing toward the graphene sheet, referred to as one-legged and two-legged, respectively. We

find the one-legged structure to be more stable by 0.014 eV in good agreement with the 0.02 eV found in a previous calculation [31] using vdW-DF2 but with the C09 exchange functional [47]. The corresponding equilibrium distance of the oxygen atom from the graphene is 3.394 in our calculations and 3.423 in Ref. 31. However, our calculation gave an angle of 30.9° away from the vertical for the O-H bond pointing toward the graphene sheet. If this O-H bond is constrained to be in the vertical plane with the bond pointing toward the graphene carbon atom, the optimized structure is less stable by approximately 0.007 eV. Upon releasing the constraint, the convergence criteria we use allows the optimization to reach the lowest energy one-legged geometry starting from the geometry with vertical O-H bond. This small difference in energy which leads to a significant difference in the predicted geometries arises from the different exchange functionals used, and seems an interesting issue for future work. In the case of the adsorbed dimer, we also find two stable structures, again one-legged and two-legged as illustrated in Fig. 1. In this case the two-legged structure is more stable by approximately 0.048 eV although the lateral position and the molecular plane of the water molecule with the two OH-bonds directed toward graphene is not the same as that for the two-legged monomer. The molecular plane of the two-legged monomer is perpendicular to the graphene plane while the molecular plane here is approximately 38° from the vertical.

For trimers, tetramers, and pentamers, we search for stable structures using an initial structure with one O-H bond pointing to a graphene carbon. For trimers and pentamers the number of O-H groups perpendicular to the approximately planar ring formed by the oxygen atoms, are different on the two sides of the ring. We search for stable structures for both orientations. The lateral position and the relative energies of the stable structures found are summarized in Fig. 1. Two general observations can be made for trimers to pentamers. First, in all stable structures the water molecules are approximately located over the hole sites of the graphene lattice. Second, the orientation with fewer O-H bonds pointing toward the adsorbing graphene sheet is favored. In the trimer, our calculations predict the one-legged orientation is more stable than the two-legged one by a very small 0.001 eV In the case of the pentamer, the two-legged orientation is more stable than the tree-legged one by 0.020 eV. For the tetramer, both orientations are two-legged. However, we examine two different structures, one with the two O-H bonds on adjacent water molecules, and one with the two O-H bonds on alternating water molecules in the cluster. These are illustrated in the right and left panels, respectively, for the tetramer in Fig. 1. The latter is more stable by approximately 0.017 eV. In our discussions below the structures shown in the left panel are used as the initial structures in geometry optimization as the graphene sheets are brought closer.

The hexamers are more complicated because a few different stable structures are available. In the gas phase as seen above, the lowest energy structures within 1 kcal/mol of each other are the prism, cage, book, and ring geometries. For the adsorbed phase we obtained five stable adsorption structures in order of increasing energy: the book, ring, cage, end-on prism, and side-on prism configurations as illustrated in Fig. 2. The two prism structures differ in their

orientation relative to the graphene sheet and thus the prism face that interacts with the graphene lattice. The book form is the most stable, and the energies of the other structures relative to this are: ring 4 meV; cage 164 meV; end-on prism 177 meV; side-on prism 209 meV. The order of stability of the hexamers in the adsorbed phase is quite different compared with the gas phase, and the relative energies span a significantly greater range for the adsorbed structures than for the gas phase structures. These results suggest the following about water cluster adsorption on graphene. In the gas phase, more compact structures allowing for greater hydrogen bonding within the cluster are favored over more open ones, as indicated in the gas-phase results for the interaction energies $E_{int,6}$ discussed above. On the other hand, adsorption interactions with the graphene surface increases with a more open structure although not changing the intracluster interactions by much, considering the intracluster bond lengths. Thus, the van der Waals interaction with graphene plays a significant role in the relative stability of the different adsorbed configurations for the hexamer.

Some structural parameters and energy for the most stable adsorption structure for each cluster size are summarized in Table 2. For the hexamer, because the energies of the ring and book form are rather close for the adsorbed cluster, we will examine the effect of graphene squeezing for both these structures calculated using vdw-DF2 (PW86). We first examine adsorption on a single-layer of graphene, simulated using a supercell with an interlayer distance of 20 Å; the results for smaller interlayer distances will be discussed below. For each density functional theory exchange-correlation functional, the average O-O distance for each adsorbed cluster is only slightly different from the corresponding gas-phase cluster. There is no clear trend, in some cases the adsorbed cluster having slightly longer O-O distances and in other cases the reverse is true. However, in most cases, the difference is smaller than 0.05 Å. The largest difference is 0.09 Å for the dimer calculated using vdw-DF (rPBE). The O-H---O bond angles differ by approximately 2° from the gas phase structure. Thus adsorption on graphene does not greatly distort the structure of water clusters as is expected for the van der Waals interaction. It is instructive to compare the structures of the adsorbed and the gas-phase clusters. Adsorption "flattens" the hexamers and the pentamer, this being clearly seen by considering the heights of the oxygen atoms in the last two rows of each entry in Table 2. For smaller clusters, this is not the case. In the book hexamer, for instance, calculated using vdw-DF2 (PW86), the oxygen atoms of the water molecules are at distances between 3.31 Å and 3.48 Å from the graphene sheet, i.e., within a 0.17 Å spread. The corresponding spread in position of the oxygen atoms in the gas-phase hexamer is 1.08 Å. For the gas-phase cluster this spread in the height of the oxygen atoms is calculated by identifying the axis along which this position spread is minimized. This can also be seen in the orientation of the O-H bonds that form hydrogen bonds in the adsorbed clusters. As an indicator, for the pentamer hydrogen-bonding O-H bonds are within 2° of a plane parallel to the graphene sheets. This "flattening" of the clusters is consistent with the layered structure that has been observed in molecular dynamics simulations of confined liquid water [8-10]

For each cluster, we calculate the cluster adsorption energy$E_{clus,N} = [E_{gas,N} + E_{grap} – E_N]$, where $E_{gas,N}$, E_N, and E_{grap} are the total energies of a gas-phase cluster, an adsorbed cluster plus graphene, and clean graphene, respectively. Thus, $E_{clus,N}$ is the energy required to form a gas-phase cluster from an adsorbed cluster. The cluster adsorption energies obtained along with some geometric parameters are tabulated in Table 2. For the monomer, we obtained adsorption distances and energies of3.39 Å and 0.113 eV for vdw-DF2 (PW86), 3.41Å and 0.116 eV for vdw-DF2 (BLYP), and 3.47Å and 0.125 eV for vdw-DF (rPBE). These results, particularly the adsorption distances, compare well with similar vdw-DF2 calculations using the C09 exchange functional exchange functional [47] which gave an adsorption distance of 3.432 Å and adsorption energy of 0.121 eV [31], although as discussed above we obtain a orientation for the monomer relative to the graphene surface. A more recent calculation that corrects for van der Waals interactions through maximally localized Wannier functions interacting as quantum harmonic oscillators give adsorption energy and distance of 0.113 eV and 3.38 Å [48]. Thus, the energies and bonding distances obtained here, particularly for vdw-DF2 (PW86), are in good agreement with previous calculations, at least for the monomer. For the larger clusters, the cluster adsorption energy $E_{clus,N}$ increases approximately linearly with cluster size as might be expected from the mostly dispersive nature of the interaction between the clusters with graphene. The vdw-DF2 (PW86) functional predicts $E_{clus,1}$ equal to 0.112 eV and $E_{clus,6}$ equal to 0.568 eV; see the first row of each entry in Table 2. Similar values are obtained for the other two functionals. Thus, the cluster adsorption energy per molecule $E_{clus,N}/N$ is approximately constant at slightly larger than 0.1 eV. The values predicted by vdw-DF2 (PW86) and vdw-DF2 (BYLP) are much closer to each other than to the value predicted by the vdw-DF (rPBE).

For comparison, we also computed the adsorption energy of argon using vdw-DF2 (BLYP). This is done with the same method as the water cluster calculations except that we use a norm-conserved pseudopotential [30]. We obtain adsorption energy of 0.111 eV and a bond length of 3.44 Å. The argon adsorption energy is in good agreement with recent density functional theory calculations that give adsorption energy of 0.112 eV and bond length of 3.49 Å [48]. The experimental results are 0.99±0.04 eV and 3.0±0.1 Å [49]. Our results show that the water monomer and argon bind to graphene with rather similar energies, as has been found previously. It has been observed that in comparison to other small molecules such as He, H_2, N_2, and Ar, rapid transport of water occurs through graphene oxide membranes with the interlayer distances between the graphene larger than 7 Å [13]. This has been suggested to be due to capillarity. Given the adsorption energies calculated here and from previous studies, this rapid transport of watercannot be due solely to the interaction of water molecules with graphene since argon has a rather similar interaction, at least when the interlayer distance is large. We will examine below the dependence of this interaction upon the interlayer distance for both water and argon.

We also calculate for the adsorbed cluster the dissociation energy $E_{diss,N}$ in a similar way as defined above for gas-phase cluster. Results are tabulated in the third row in each set of values in Table 2. As discussed above, $E_{diss,N}$ provides a gauge of the intermolecular interactions in the

adsorbed clusters. The hydrogen-bond strength between two adsorbed water molecules is 0.252 eV compared to the 0.244 eV for the gas-phase. Close similarity with results for the gas-phase clusters is expected since we have seen that the adsorption only slightly changes the structure of the cluster. Thus, just as for the gas phase, it is easier to dissociate one adsorbed water molecule from a pentamer than from either a tetramer or a hexamer, for the adsorbed cluster. For clusters larger than the dimer, the dissociation energy is only slightly decreased by adsorption, this decrease being smaller than approximately 0.05 eV compared to the gas-phase cluster. The adsorbed dimer has $E_{diss,N}$ larger than the gas phase by 0.03 eV. These similar trends in the results for the adsorbed and gas phase cluster show that adsorption only has a small influence on the cluster geometry and the interactions between the water molecules in it. From these results, we expect $E_{diss,N}$ to increase to the bulk value as the cluster size grows beyond the hexamer because the clusters will become more 3-dimensional and the number of hydrogen bond per molecule increases, consequently increasing the intermolecular interaction. This interaction generally increases with cluster size reaching approximately 0.5 eV for the hexamer. Thus, there is a significant amount of cohesion within adsorbed water clusters at room temperature. We next examine how this cohesion depends upon the interlayer distance between the graphene sheets.

In order to assess the adsorption energy relative to gas-phase water molecules, we also calculate the molecular adsorption energy $E_{mol,N} = [NE_{gas,1} + E_{grap} - E_N]/N$ for each cluster as a function of the interlayer distance. For the hexamer, results for the book form and the more open ring form are shown. It is instructive to reference this to the molecular adsorption energy at large interlayer distance d, which in our calculations we take as the d= 20 Å case, that is $E_{rel,N}(d) \cong E_{mol,N}(d) - E_{mol,N}(20)$. To our knowledge, there are no previous first-principles calculations to compare our results against. The dependence of the relative adsorption energy upon the interlayer distance d for each cluster size is plotted in Fig. 3. Clearly, $E_{rel,N}(d)$ goes to zero as the interlayer distance increases. For instance, $E_{rel,N}(13)$ for vdw-DF2 (PW86), vdw-DF2(BLYP), and vdw-DF (PBE) are already quite small, approximately 0.0014, 0.0022, and 0.0028 eV, respectively. This provides some validation for using results from the d = 20 Å simulations as the limit of large interlayer distance in our analysis. From the results in Fig. 3 we can see that as d decreases, the adsorption energy increases to a maximum at d between 6.5 and 7 Å, this distance depends only slightly upon the density functional used, and is approximately equal to twice the adsorption distances for d = 20 Å. Thus, the maximum in $E_{rel,N}(d)$ is likely mostly due to the van der Waals interactions of the water molecules with both confining graphene sheets, giving maximum values of approximately 0.11 eV to 0.15 eV. It decreases slightly with cluster size. For all three functionals $E_{rel,1}(d)$has a slightly larger maximum of 0.15 eV for the monomer compared to the larger clusters which have approximately the same maximum value of 0.10 eV.

Our results show that adsorption within multilayer graphene, with an interlayer distance of approximately 6 Å, is slightly favored over adsorption on a single graphene sheet for larger interlayer distances. Similar behavior is also observed for argon adsorption, with a maximum in

$E_{rel,1}(d)$, also of approximately 0.1 eV and also for a similar interlayer distance d about 6 Å. At these maxima in $E_{rel,N}$ the clusters are approximately halfway between the graphene sheets. Thus, this maximum in $E_{rel,N}(d)$ is due to the van der Waals interactions with both graphene sheets confining the cluster. For interlayer distances smaller than about 6 Å, adsorption becomes greatly unfavorable. The adsorption energy dependence upon interlayer distance for water and argon are quite similar; the adsorption energy maxima are of similar magnitudes and occur at similar interlayer distances. Thus, the physisorption of gases into graphene membranes can be enhanced by controlling the interlayer distance between the graphene sheets. This is potentially useful in increasing the sensitivity of gas detection through adsorption on graphene.

We also examine the interaction of water clusters through the graphene sheets with the vdw-DF2 (PW86) method. Using the pentamer, we performed initial calculations to compare the relative stability of two orientations of the cluster, with dipoles oriented parallel or anti-parallel. For an interlayer distance of 6 Å, the former is found to have a lower energy, and subsequent calculations for all clusters are performed for parallel dipole orientations. For large interlayer distances, this interaction decreases to zero as expected. We find a maximum of about 0.06 eV for interlayer distance d at approximately 6 to 7 Å. With this additional interaction between water clusters trapped between adjacent interlayer spaces, the adsorption energy maximum in $E_{rel}(d)$ is increased to approximately 0.16 eV. Thus, with multilayers of water adsorbed between the graphene sheets, the adsorption energy for each cluster increases slightly, at least for interlayer distances larger than about 6 Å.

In order to further examine the effect of interlayer distance upon the energetics, we calculate the dissociation energy $E_{diss,N}(d)$ as a function of interlayer distance. We have discussed $E_{diss,N}$ above for the case of large interlayer distance. This is the energy needed to dissociate an adsorbed N-molecule cluster into an adsorbed (N-1)-molecule cluster and an adsorbed water molecule, all at the same interlayer distance. For the gas-phase dimer the values of $E_{diss,2}(20)$ are 0.244, 0.238, and 0.214 eV, for the vdw-DF2 (PW86), vdw-DF2 (BLYP), and vdw-DF1 (rPBE), respectively. The adsorbed case has the corresponding $E_{diss,2}(20)$values equal to 0.274, 0.261, and 0.238 eV for an interlayer distance of 20 A. Thus, we conclude that adsorption on graphene slightly increases the hydrogen-bond interactions between water molecules. The results for different cluster sizes and interlayer distances are shown in Fig 4. It is clear that as the interlayer distance decreases, $E_{diss,N}(d)$ begins to decrease sharply for d smaller than approximately 6 to 8 Å, depending slightly on cluster size. The book hexamer calculations with vdw-DF (rPBE) shows a decrease in $E_{diss,N}(d)$ even for d=13 A, but for the vdw-DF2 (PW86) and vdw-DF2 (BLYP) calculations, $E_{diss,N}(d)$ is constant until d is smaller than about 8 Å. For the hexamer, we also plot results for the ring structure. As can be seen, the decrease in $E_{diss,6}$ at small interlayer distances and the value of $E_{diss,6}$ itself are considerably lower for the ring structure than the book structure, the dissociation energy by almost 0.2 eV. We can understand this because the dissociation energy is a measure of the hydrogen bonding interaction within the cluster, and is thus higher for the more compact book structure. We also note that the behavior of the dissociation energy with squeezing

for the ring hexamer is, expectedly, similar to that of the (ring) pentamer. As we have seen above, the pentamer has a smaller $E_{diss,N}(d)$ than the tetramer. This is because of the unfavorable hydrogen bond angles in the trimermaking the tetramer particularly difficult to dissociate and consequently a high $E_{diss,4}$. The book hexamer is three dimensional. This is interesting here because, as we have seen above, adsorption leads to a flattening of the hexamer. As d decreases, $E_{diss,N}(d)$ decreases most rapidly for the book hexamer compared to the smaller clusters. This behavior can be contrasted with that for the ring hexamer for which the decrease is closer to that shown by the smaller clusters. This is probably due to the change from a three-dimensional structure to a flatter one for the book hexamer, in contrast to the ring hexamer and to the smaller clusters where the oxygen atoms are all approximately in the same plane even for the gas phase. Thus, squeezing the three-dimensional hexamers involves a larger change in shape and stability. We expect the same behavior when squeezing liquid water. It has been previously found that the transport of water molecules through carbon nanotubes takes place by a mechanism whereby a single row of water molecules move through the nanotube in single file [2]. Intermolecular hydrogen bonding between consecutive water molecules is important in that mechanism. From our data it is apparent that as the interlayer distance decreases, the hydrogen bond interactions begins to decrease significantly when d becomes smaller than 8 Å. We argue that the motion of liquid water when squeezed between graphene sheets also depend strongly upon the intermolecular hydrogen bonds. Given a mechanism whereby water molecules move through the space between graphene sheets in a concerted fashion because of this hydrogen-bonding just as in the single-file transport through carbon nanotubes, a decrease in the bonding would reduce the transport rate. We did not attempt to calculate the interaction energies of argon clusters as this is not within reasonable reach of the method used here. However, similar behavior to water clusters is not expected. Thus, our results are consistent with the experimental observation of rapid transport of water, in contrast to other small molecules like argon for example, through graphene oxide membranes. The strong intermolecular interactions between the water molecules persist until the interlayer distance drops below approximately 6 to 8 Å.

Finally, we also calculate the lateral corrugation in the adsorption potential in order to quantify the energy barrier for sliding water along the graphene sheet. In order to simulate the layered structure that has been suggested for liquid water confined between graphene sheets, we perform these calculations for the pentamer, which is the largest “flat” gas-phase cluster studied here. The results are shown in Fig. 5a. We used the nudged-elastic band method between the two geometry-optimized structures at the end-points of the path illustrated in the inset of Fig. 5a.In Figs. 5b to 5d, we plot the potential energy along this path for different interlayer distances. It is clear that the corrugation increases dramatically when the interlayer distance decreases below approximately 6 Å. For interlayer distances larger than 6.5 Å, the maximum barrier height for sliding a pentamer along the graphene sheet is less than 0.03 eV. Thus, the graphene corrugation is not important at room temperature for diffusive motion of adsorbed clusters along the graphene sheet. This barrier approximately doubles for every 0.5 Å decrease in the interlayer distance, reaching a value of 0.33 eV for 5 Å. In combination with the results above for $E_{diss,N}$,

we conclude that for interlayer distances smaller than about 6 Å, stick-slip motion of water occur. At larger interlayer distances we have hydrogen-bond mediated concerted motion with little influence from the small potential energy corrugation of graphene.

Conclusions

We have investigated the intermolecular interactions within small water clusters up to the hexamer, and the adsorption of these clusters on the confining graphene sheets. Our gas-phase cluster energetics and structures show that the accuracy of the faster vdw-DF methods are in reasonable agreement with more sophisticated quantum chemical calculations. The intermolecular interaction energy E_{int} are within 0.05 eV of MP2-CBS calculations [33]. The vdw-DF2 calculations give higher interaction energies than MP2-CBS while vdw-DF interaction energies are all lower than MP2-CBS results. The average bond length is within 0.15 Å and the average O-H---O bond angle is within 6° of DCACP results [36]. The bond lengths from vdw-DF are all overestimated compared to the DCACP calculations, with the vdw-DF2 (PW86) giving the best agreement. The energy ordering of the gas-phase hexamers predicted by previous work using quantum chemical methods is reproduced by the vdw-DF2 (PW86) calculations. The difference in the dissociation energies predicted for these hexamers by the vdw-DF2 (PW86) method used here and the ΔCCSD(T) method is between 14 meV and 17 meV. The adsorbed hexamers are ordered differently in energy showing that van der Waals interaction with the graphene plays an important role in determining the relative energies of the different hexamers – in particular, the open ring hexamer is significantly more stabilized upon adsorption than the more compact hexamers.

To quantify the van der Waals interaction between the cluster and graphene we calculate the cluster adsorption energy per water molecule in the cluster. This is approximately constant at about 0.1 eV/molecule. Thus, as the cluster size increases, the energy required to desorb a cluster increases from about 0.112 eV for the monomer to 0.568 eV for the hexamer. These are results from vdw-DF2 (PW86), but results from the other two functionals used are similar. Hexamers and pentamers, and presumably larger adsorbed clusters are "flatter" than gas-phase clusters. The O-H bonds in the hydrogen-bonded hydroxyls are almost parallel to the graphene plane. This is consistent with molecular dynamics results that show layer-by-layer structure near graphene sheets [8-11].To make a connection to gas-phase water molecules, we also calculate the molecular adsorption energy which is the energy required to form gas-phase molecules rather than gas-phase clusters from adsorbed clusters. We find a maximum in the adsorption energy of approximately 0.15 eV at interlayer distances about 6 to 7 Å arising from interactions with both graphene sheets. Thus, squeezing water clusters between graphene sheets increases the adsorption energy, at least for interlayer distances larger than about 6 Å. This maximum is not large but significant enough to affect the adsorption capacity at not too low temperatures. Since

this is due to van der Waals interactions, the maximum should be observed for any molecule that physisorbs on graphene.

We also quantify the intermolecular interaction in the cluster for both gas-phase and adsorbed clusters by calculating a dissociation energy $E_{diss,N}(d)$ which depends upon the cluster size and distance. For the dimer $E_{diss,2}$ provides the hydrogen-bond strength between two water molecules. For larger clusters $E_{diss,N}$ is the energy required to dissociate the N-molecule cluster to form a (N-1)-molecule cluster and a molecule of water. We obtain slightly stronger hydrogen bonds in the adsorbed dimers than in the gas phase. While $E_{diss,N}$ is a probe of the hydrogen bonding within the clusters, its valuefor any cluster is not simply proportional to the change in the number of hydrogen bonds upon dissociation. This is because the hydrogen-bond geometry, and thus the bond strength, in these small clusters depend upon the cluster size. For the pentamer, a dip in $E_{diss,N}$ is found, that is the tetramer and the hexamer have higher dissociation energies than the pentamer. In the case of the tetramer this arises from the trimer being particularly unstable, and in the case of the hexamer, this arises because of the increase in the number of hydrogen bonds per molecule in the hexamer compared to the pentamer. For interlayer distances larger than approximately 8 Å, $E_{diss,N}$ does not change significantly. However, for smaller interlayer distance, approximately 6 to 8 Å depending upon the cluster size, $E_{diss,N}$ decreases sharply with the interlayer distance. We show that this decrease is particularly large for the book hexamer compared to the smaller clusters and to the ring hexamer, and is likely due to the greater decrease in the intracluster hydrogen bonding as the more 3-dimensional book hexamer is squeezed compared to the more ring structures for the smaller clusters and the ring hexamer. Thus, the confinement of water clusters within graphene sheets closer than about 6 to 8 Å significantly decreases the attractive interactions between the water molecules. These results support a model of water transport through graphene membranes where the motion of the water molecules is concerted because of the hydrogen-bonding between them. Our results are consistent with this picture of the observed rapid transport of water through graphene oxide membranes, and with the large decrease in this transport rate observed when the interlayer distance decreases to approximately 7 Å. Thus, our results provide molecular scale evidence for the idea that hydrogen-bonding is responsible for the rapid flow of water through graphene oxide membranes [10]. We also calculate the corrugation potential as a function of the interlayer distance. This is small at less than 0.03 eV for interlayer distances larger than 6.5 Å, but increases rapidly upon further confinement.

In summary, we have found that the confinement of water clusters between graphene sheets with nanoscale interlayer distances leads to interesting effects on the molecular interactions. First, we observe a maximum in the adsorption energy as the interlayer distance is reduced. This is due to the van der Waals interactions with graphene. Second, squeezing water clusters between graphene also leads to weakening of the hydrogen-bond interactions between the water molecules. This occurs as the interlayer distance decreases below approximately 6 to 8 Å depending upon cluster size. These molecular effects should provide insight into understanding

the interactions of water trapped in graphene membranes, and potentially have impact the design and fabrication of materials for nanoscale separations.

References

1) A.I. Kolesnikov, J.M. Zanotti, C.K. Loong, P. Thiyagarajan, A.P. Moravsky, R.O. Loutfy, and C.J. Burham. Phys. Rev. Lett.**93**, 035503 (2004).
2) G. Hummer, J.C. Rasalah, and J.P. Nowortya, Science **414**, 188 (2001).
3) J.K. Holt, H.P. Park, Y. Waang, M. Stadermann, A.B. Aryukhin, C.P. Grigopoupulos, A. Noy, and O. Bakajin, Science**312**, 1034 (2006).
4) M. Majumder, N. Chopra, R. Andrews, and B.J. Hinds, Nature**438**, 44 (2005).
5) N. Naguib, H. Ye, Y. Gogotsi, A.G. Yazicioglu, and C.M. Constantine, Y. Masahiro Nano Lett.**4**, 2237 (2004).
6) R.C. Major, J.E. Houston, M.J. McGrath, J.I. Siepmann, and X.Y. Zhu, Phys. Rev. Lett. **96**, 177803 (2006).
7) N. Choudhary and B.M. Pettitt, J.Phys. Chem B **109**, 6422 (2005).
8) J. Marti, G. Nagy, M.C. Gordillo, and E. Guàrdia, J. Chem. Phys.**124**, 094703 (2006).
9) S.A. Deshmukh, G.Kamath, G.A. Baker, A.V. Sumant, and S.K.R.S. Sankaranarayanan, Surf. Sci. 609, 129 (2013).
10) G. Cicero, J.C. Grossmann, E. Schwegler, F. Gygi, and G. Galli, J. Am. Chem. Soc.**130**, 1871 (2008).
11) N. Giovambattista, P.J. Rossky, and P.G. Debennetti, Phys. Rev. Lett. **102**, 050603 (2009).
12) R. Zangi andA.E. Mark, Phys. Rev. Lett. **91**, 025502 (2003).
13) R.R. Nair, H.A. Wu, P.N. Jayaram, I.V. Grigorieva, and A.K. Geim, Science **335**, 442 (2012).
14) K. Raidongia and J.X. Huang, J. Am. Chem. Soc.**134**, 16528 (2012).
15) P.Z.P. Sun, M. Zhu, K. Wang, M. Zhong, J. Wei, D. Wu, Z. Xu, and H. Zhu, ACS Nano **7**, 428 (2013).
16) J.C. Rasaiah, S. Garde, and G. Hummer, Annu. Rev. Phys. Chem.**59**, 713 (2008).
17) M. Dion, H. Rydberg, E. Schröder, D.C. Langreth, and B.I. Lundqvist, Phys. Rev. Lett. **92**, 246401 (2004).
18) K. Lee, E.D. Murray, L. Kong, B.I. Lundqvist, and D.C. Langreth, Phys. Rev. B **82**, 081101(R) (2010).
19) M. Elstner, P. Hobza, T. Frauenheim, S. Suhai, and E. Kaxiras, J. Chem. Phys.**114**, 5149 (2001).
20) S. Grimme, J. Antony, S. Ehrlich, and H. Krieg, J. Chem. Phys.**132**, 154104 (2010).
21) P. Jurecka, J. Cerny, P. Hobza, and D.R. Salahub. J. Comput. Chem **28**, 555 (2007).
22) A.J. Misquitta and K. Szalewicz, Chem. Phys. Lett. **357**, 301 (2002).
23) A. Hesselmann, G. Jansen, and M. Schutz, J. Chem. Phys. **122**, 014103 (2005).
24) P. Giannozzi, et al, The Quantum-ESPRESSO package; http://dx.doi.org/10.1088/0953-8984/21/39/395502 (2009).
25) J. Klimes, D.R. Bowler, and A. Michealides, J.Phys. Cond. Mat. 22, 022201 (2010).

26) J.P. Perdew, K. Burke, M. Ernzehof, Phys. Rev. Lett. **77**, 3865 (1996); Phys. Rev. Lett. **78**, 1396 (1997).
27) A.D. Becke, Phys. Rev. A **38**, 3098 (1988); C. Lee, W. Yang, R.G. Parr, Phys. Rev. B **37**, 785 (1988).
28) J.P. Perdew and W. Yue, Phys. Rev. B **33**, 8800 (1986).
29) A.M. Rappe, K.M. Rabe, E. Kaxiras, J.D. Joannopoulos, Phys. Rev. B **41**, 1227 (1990).
30) S. Goedecker, C. Hartwigsen, J. Hutter, Phys. Rev. B **58**, 3641 (1998); S. Goedecker, M. Teter, J. Hutter, Phys. Rev. B **54**, 1703 (1996).
31) I. Hamada, Phys. Rev. B **86**, 195436 (2012).
32) J. Ma, A. Michaelides, D. Alfè, L. Schimka, G. Kresse, and E. Wang, Phys. Rev. B **84**, 033402 (2011)
33) S.S Xantheas, C.J. Burnham, and R.G. Harrison, J. Chem. Phys.**116**, 1493 (2002).
34) A.K. Kelkkanen, B.I Lundqvist, and J.K. Nørskov, J. Chem. Phys.**131**, 046102 (2009).
35) P.L. Silvestrelli, Chem. Phys. Lett.**475**, 285 (2009).
36) B. Santra, A. Michaelides, M. Fuchs, A. Tkatchenko, C. Filippi, and M. Scheffler, J. Chem. Phys. **129**, 194111 (2008)
37) F.F. Wang, G. Jenness, W.A. Al-Saidi, and K.D. Jordan, J. Chem. Phys. **132**, 134303 (2010).
38) M.J. Gillan, D. Alfè, A.P. Bartók, G. Csányi, J. Chem. Phys. **139**, 244504 (2013).
39) I. Lin, A.P. Seitsonen, I. Tavernelli, and U. Rothlisberger, J. Chem. Theo. Comput.**8**, 3902 (2012).
40) M. Rubeš, P. Nachtigall, J. Vondrašek, and O. Bludský, J. Phys. Chem. C **113**, 8412 (2009)
41) E. Voloshina, D. Usvyat, M. Schütz, Y. Dedkov, and B. Paulus, Phys. Chem. Chem. Phys. **13**, 12041 (2011).
42) J. Kysilka, M. Rubeš, L. Grajciar, P. Nachtigall, and O. Bludský, J. Phys. Chem. A **115**, 11387 (2011).
43) H. Li and X.C. Zeng, ACS Nano **6**, 2401 (2012).
44) S. Yoo, S.S. Xantheas, J. Chem. Phys. **134**, 121105 (2011).
45) S. Grimme, J. Comput. Chem. **27**, 1787 (2006).
46) G. Cicero, J.C. Grossman, E. Schwegler, F. Gygi, and G. Galli, J. Amer. Chem. Soc. **130**, 1871 (2008).
47) V.R. Cooper, Phys. Rev. B **81**, 161104(R) (2010).
48) P.L. Silvestrelli, A. Ambrosetti, J. Chem. Phys.**140**, 124107 (2014).
49) G. Vidali, G. Ihm, H.Y. Kim, and M.W. Cole, Surf. Sci. Rep. **12**, 135 (1991).

Table 1

Results for gas-phase clusters obtained in our calculations are comparedto results from two previous calculations. For each set of values in the table, the first row is the interaction energy $E_{int,N}$ in eV. The numbers in the second row are, respectively, the average O-O distance L in Å and the average O-H---H angle θ for the hydrogen bonds in each cluster; no geometric data is available for the MP2-CBS calculations. The third row in each set is the dissociation energy$E_{diss,N}$ in eV.

[1] Ref. 39; [2] Ref. 33

	dimer	trimer	tetramer	pentamer	hexamer(book)
vdw-DF2 (PW86)					
$E_{int,N}$	0.244	0.702	1.230	1.626	2.076
L, θ	2.947,176.6°	2.829,149.8°	2.781,166.6°	2.762,175.2°	2.879,165.1°
$E_{diss,N}$	0.244	0.458	0.528	0.396	0.450
vdw-DF2 (BLYP)					
$E_{int,N}$	0.238	0.685	1.208	1.594	2.040
L, θ	2.978,177.0°	2.848,150.4°	2.787,166.4°	2.872,175.8°	2.884,165.2°
$E_{diss,N}$	0.238	0.447	0.523	0.386	0.446
vdw-DF (rPBE)					
$E_{int,N}$	0.214	0.610	1.108	1.489	1.997
L, θ	3.020,175.7°	2.866,149.9°	2.806,166.6°	2.771,175.1°	2.919,164.9°
$E_{diss,N}$	0.214	0.396	0.498	0.381	0.508
DCACP-BLYP[1]					
$E_{int,N}$	0.230	0.722	1.289	1.686	2.129
L, θ	2.92,170.3°	2.81,151.1°	2.75,168.3°	2.72,176.3°	2.73,168.8°
$E_{diss,N}$	0.230	0.492	0.567	0.397	0.443
DCACP-rPBE [1]					
$E_{int,N}$	0.226	0.724	1.299	1.716	2.118
L, θ	2.88,170.6°	2.78,152.2°	2.72,168.6°	2.69,176.4°	2.71,169.0°
$E_{diss,N}$	0.226	0.498	0.575	0.417	0.402
MP2/CBS [2]					
$E_{int,N}$	0.216	0.686	1.198	1.573	2.033
L	2.91	2.79	2.73		
$E_{diss,N}$	0.216	0.47	0.512	0.375	0.46

Table 2

Results for adsorbed clusters with interlayer distance equal to 20 Å are summarized in this table. For each set of values in the table, the first row is the interaction energy $E_{clus,N}$ in eV. The numbers in the second row are, respectively, the average O-O distance L in Å and the average O-H---H angle θ for the hydrogen bonds in each cluster. The third row in each set is the dissociation energy $E_{diss,N}$ in eV. The fourth row in each set are the smallest distance z_{min} and largest distance z_{max} in Å of the cluster oxygen atoms from the plane of the graphene. The last row are the z_{min} and z_{max} for the corresponding gas-phase cluster oxygen atom distances from an arbitrary plane calculated as explained in the text. Comparison with the adsorbed cluster results provide an assessment of the "flatness" of each cluster.

	monomer	dimer	trimer	Tetramer	pentamer	hexamer (book)
vdw-DF2 (PW86)						
$E_{clus,N}$	0.112	0.252	0.326	0.421	0.513	0.568
L, θ		2.899,178.5°	2.835,150.3°	2.788,167.3°	2.776,175.9°	2.895,1.63[illegible]°
$E_{diss,N}$		0.271	0.419	0.511	0.374	0.493
z_{min},	3.394	3.07,3.34	3.17,3.35	3.22,3.39	3.23,3.34	3.31,3.48
z_{max}(adsorbed)		4.89,5.05	4.41,4.59	4.44,4.56	4.40,4.75	4.12, 5.20
z_{min}, z_{max}(gas)						
vdw-DF2 (BLYP)						
$E_{clus,N}$	0.116	0.251	0.3212.892,150.2°	0.411	0.500	0.548
L, θ		2.988,179.7°	0.401	2.806,167.7°	2.789,175.9°	2.930,162.9[illegible]
$E_{diss,N}$		0.258	3.28,3.45	0.497	0.359	0.479
z_{min},	3.410	3.26,3.52	4.38,4.60	3.33,3.53	3.39,3.48	3.37,3.61
z_{max}(adsorbed)		4.88,5.05		4.46,4.54	4.41,4.73	4.16,5.19
z_{min}, z_{max}(gas)						
vdw-DF2 (rPBE)						
$E_{clus,N}$	0.125	0.285	0.378	0.488	0.597	0.661
L, θ		2.932,178.8°	2.855,149.9°	2.795,167.4°	2.782,176.0°	2.907,163.1°
$E_{diss,N}$		0.248	0.364	0.482	0.363	0.447
z_{min},	3.467	3.11,3.37	3.15,3.38	3.20,3.41	3.21,3.37	3.29,3.49
z_{max}(adsorbed)		4.89,5.06	4.39,4.60	4.45,4.55	4.41,5.08	4.12,5.27
z_{min}, z_{max}(gas)						

Figure 1

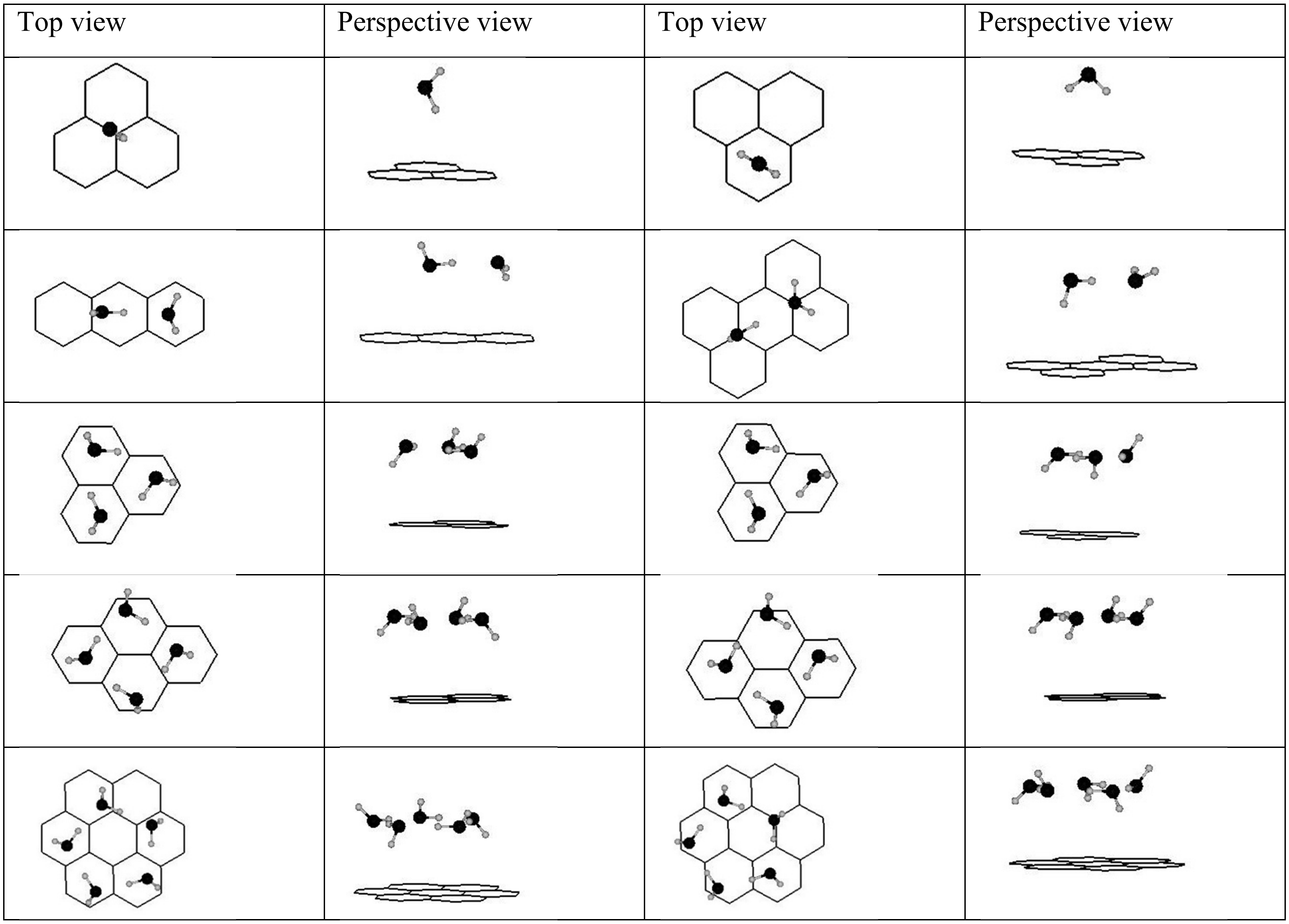

Figure 2

Hexamer	Top view	Perspective view
Book	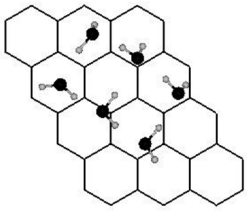	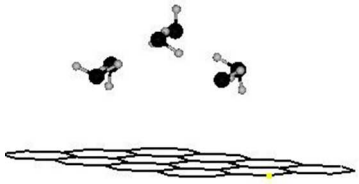
Ring	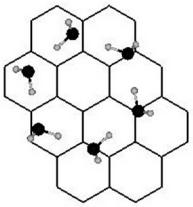	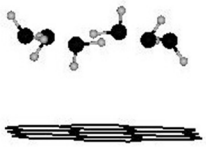
Cage	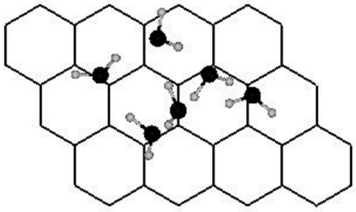	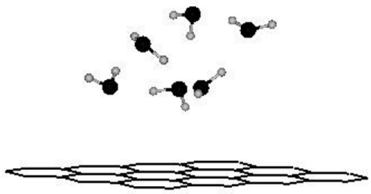
Prism-end on	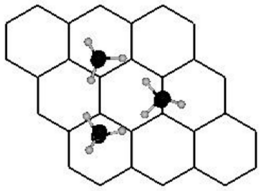	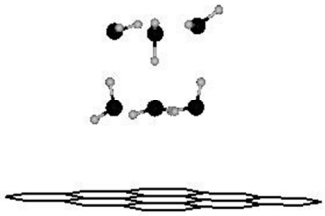
Prism-side-on	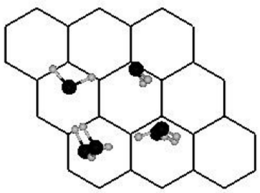	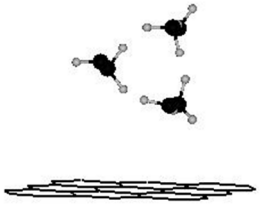

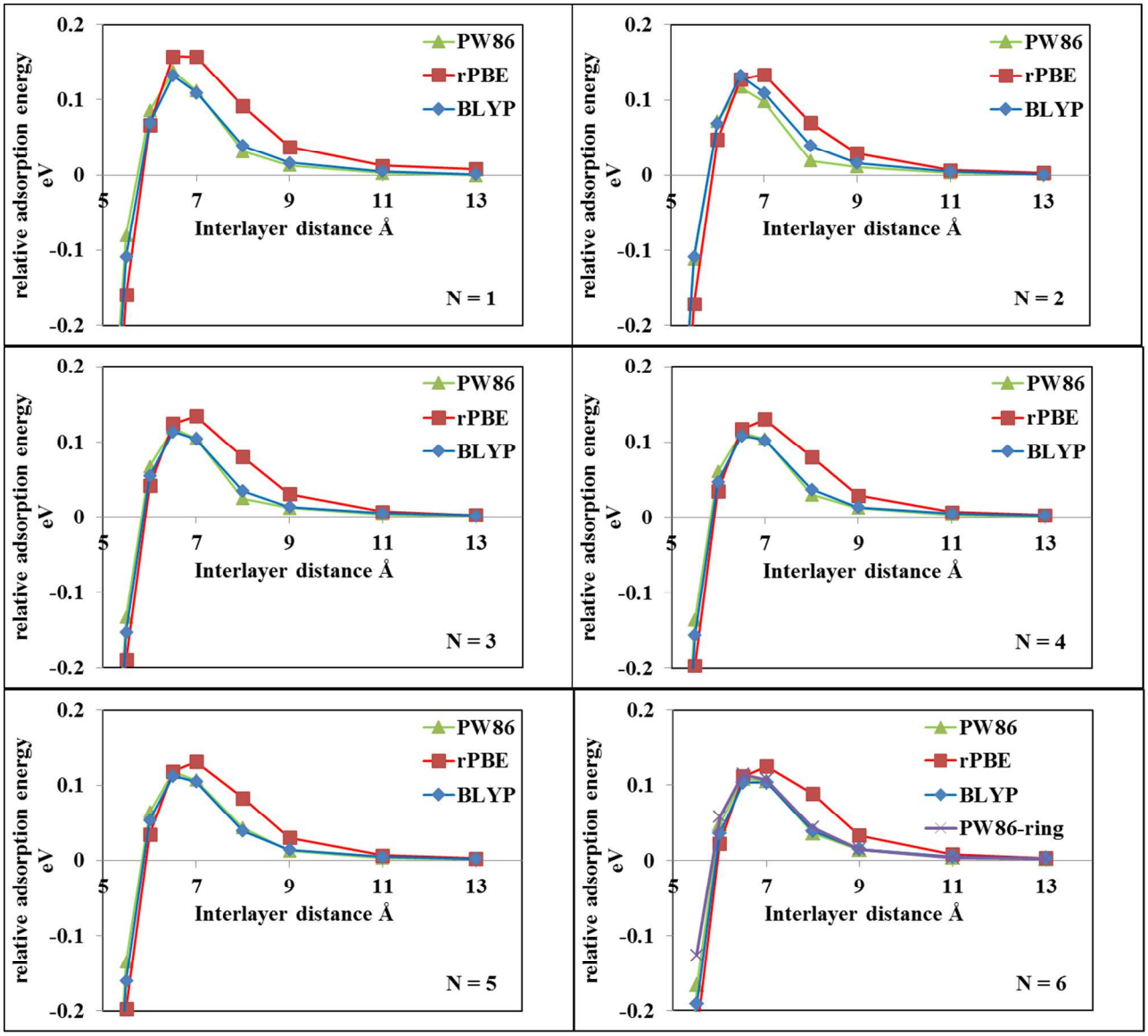

Figure 3

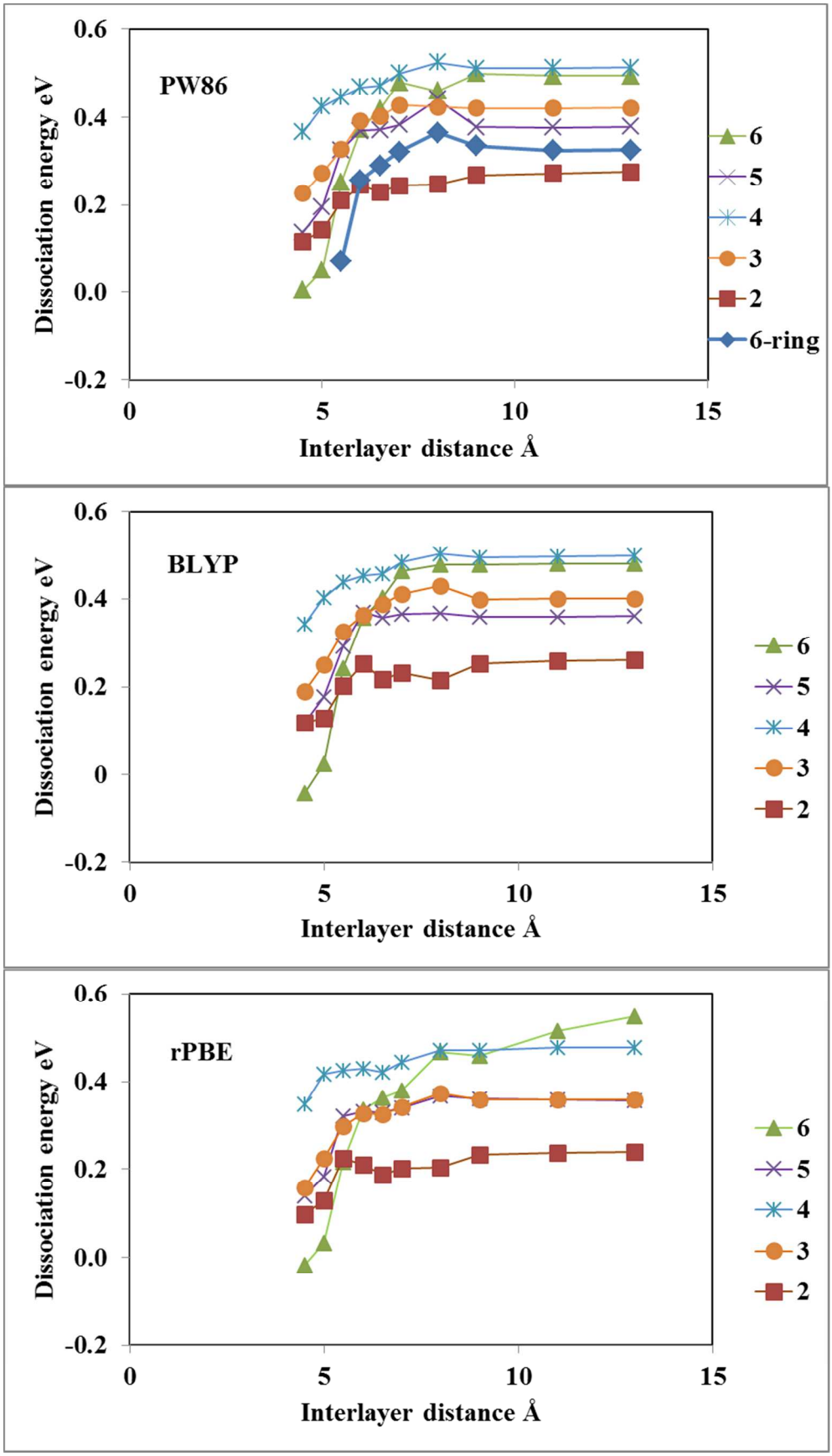

Figure 4

Figure 5

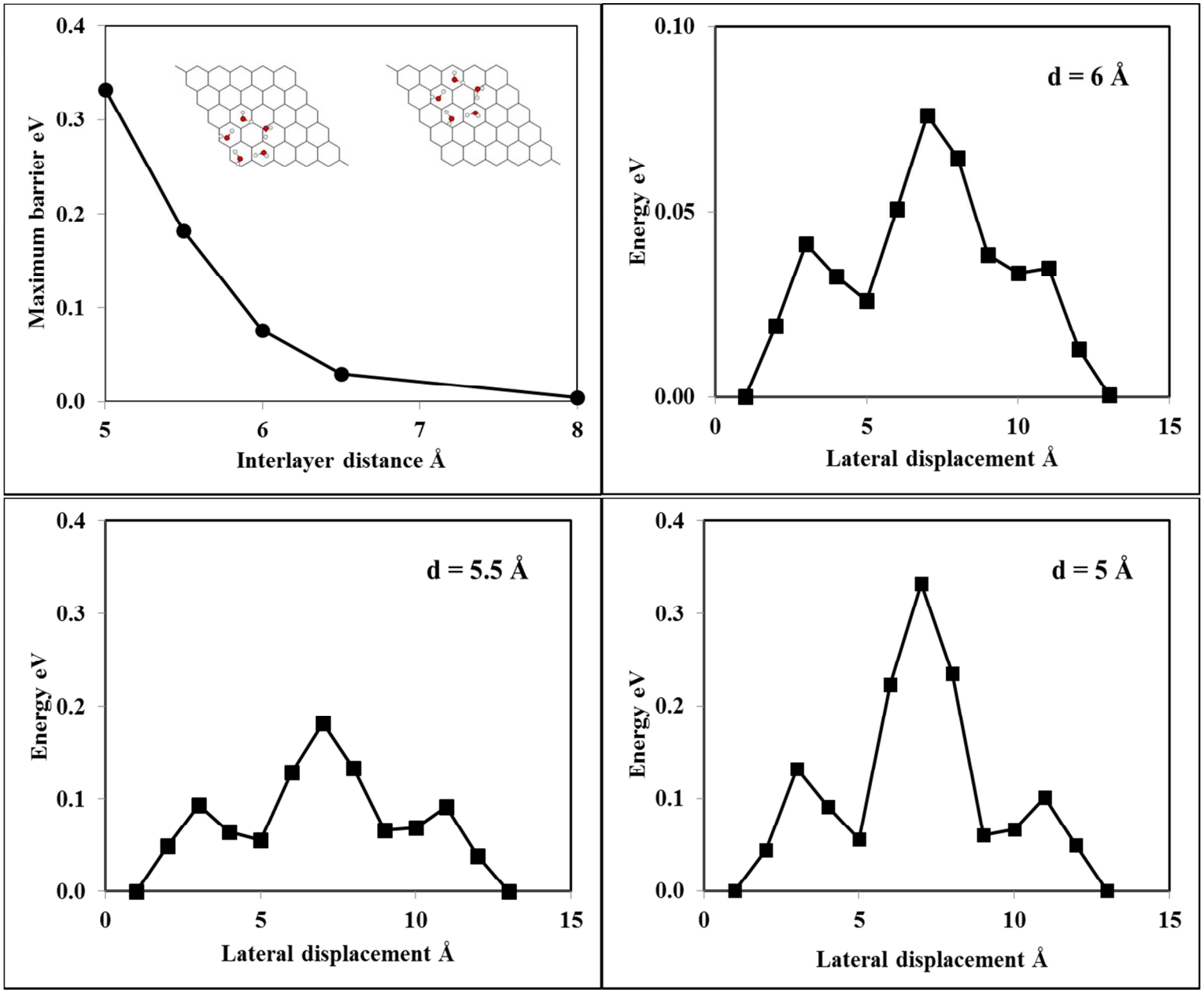

Figure Captions

Figure 1
Stable adsorption configurations of monomers to pentamers are illustrated in this figure. For each cluster size, we found two stable structures, for top and persp[erctive view for each of which is illustrated. For each cluster size, the structure shown in the left panels is the more stable. Oxygen atoms are denoted by the larger black circles, and hydrogen by the smaller gray circles.

Figure 2
The five stable adsorption configurations found for the hexamer. The structures are arranged in decreasing order of stability with most stable (book) in the top row to least stable (side-on prism) in bottom row. Top and perspective views are illustrated for each.

Figure 3
In this figure we plot the relative adsorption energy per molecule $E_{rel,N}(d)/N$ as a function of interlayer distance d. For each cluster size N, we plot the results for the three different methods used: vdw-DF2 (PW86) (green data points and line); vdw-DF2 (BLYP) (blue); vdw-DF (rPBE) (red). For the hexamer, we include results for the ring structure calculated using tvdw-DF2 (PW86). In general, it is observed that the maxima in $E_{rel,N}(d)/N$ occurs at approximately 6.5 to 7 Å; this decreases slightly with cluster size.

Figure 4
The dissociation energy $E_{diss,N}$ for adsorbed clusters is plotted here as a function of the interlayer distance d. Each panel is labeled with the exchange functional used, and shows results for different cluster sizes N. For vdw-DF2 (PW86) results for the hexamer include both the book and the ring sturctures. At large interlayer distances, $E_{diss,N}(d)$ goes to a constant; $E_{diss,2}$ is the hydrogen-bond strength between two adsorbed water molecules. For d smaller than about 8 Å, the energy $E_{diss,N}$ required to dissociate one adsorbed molecule from the adsorbed cluster decreases rapidly with d. Regardless of the vdw-DF method used, the dissociation energy for the book hexamer decreases most rapidly and by the largest amount.

Figure 5
The interaction potential between an adsorbed pentamer and the graphene sheet depends upon the lateral position of the cluster. In Fig 3a, we plot the maximum barrier height for this corrugation for the path with end-points illustrated in the inset. We plot the corrugation potentials for different interlayer distances in Figs. 3b to 3d. It can be seen that the maximum barrier height increases rapidly for interlayer distances below approximately 6 Å.